

Lymphoma cell-driven IL-16 is expressed in activated B-cell-like diffuse large B-cell lymphomas and regulates the pro-tumor microenvironment

Xuwen Guan,^{1,2,3,4*} Yi Wang,^{1,2*} Teng Fang,^{1,2} Jingya Wang,⁵ Ru Li,^{1,2} Mu Hao^{1,2} and Lugui Qiu^{1,2}

¹State Key Laboratory of Experimental Hematology, National Clinical Research Center for Blood Diseases, Haihe Laboratory of Cell Ecosystem, Institute of Hematology and Blood Diseases Hospital, Chinese Academy of Medical Sciences and Peking Union Medical College;

²Tianjin Institutes of Health Science; ³Department of Hematology, Tianjin First Central

Hospital; ⁴Department of Hematology, Nankai University Affiliated First Central Hospital and

⁵Tianjin Medical University Cancer Institute & Hospital, National Clinical Research Center for Cancer; Key Laboratory of Cancer Prevention and Therapy; Tianjin's Clinical Research Center for Cancer; Department of Thoracic Oncology, Tianjin Lung Cancer Center, Tianjin Cancer Institute & Hospital, Tianjin Medical University, Tianjin, PR China

**XG and YW contributed equally as first authors.*

Correspondence: L. Qiu
qiulg@ihcams.ac.cn

M. Hao
haomu@ihcams.ac.cn

Received: February 26, 2024.

Accepted: September 19, 2024.

Early view: September 26, 2024.

<https://doi.org/10.3324/haematol.2024.285304>

©2025 Ferrata Storti Foundation

Published under a CC BY-NC license



Supplementary methods

Mice Models

For human DLBCL cells, the NOD SCID mice were inoculated subcutaneously on the right side with a mixture containing 5×10^6 tumor cells and Matrigel (354248, BD Biosciences, San Diego, CA, USA) (1:1). For murine DLBCL cells, the BALB/c nude mice or BALB/c mice were inoculated subcutaneously on the right side with 1×10^6 tumor cells in 200 μ L PBS. When the tumors became palpable, tumor volumes (tumor volume = (length x width²)/2) and body weight were measured at an interval of 1–2 days. Further, when the tumor volume reached a particular size, based on the ethical guidelines (The maximum diameter <20 mm), the mice were anesthetized and sacrificed, and the tumor samples were collected for further analysis.

For Clodronate Liposomes (a chemical depletion of macrophages in an animal model treatment, Yeasen, China, Cat#: 40337ES10)¹, the BALB/c nude mice were randomized (completely randomized by random number table) into two groups (5 mice/group): Clodronate Liposomes or Control treatment. For detail, mice were treated with 200 μ L Clodronate Liposomes (5mg/ml, i.p.) or saline (i.p.) treatment on Day0, and then the mice were inoculated subcutaneously on the right side with 1×10^6 A20 cells in 200 μ L PBS on Day1. Furthermore, the mice were treated on Day4, 8 and Day12, and the mice were then anesthetized and sacrificed on Day16..

For IMM0306 (a fusion protein of CD20 mAb with the CD47 binding domain of SIRP α (V2) extracellular segment domain 1 (D1) on both heavy chains) treatment², when the tumors reached a mean of 200 mm³, the NOD SCID mice which bear tumors were randomized (completely randomized by random number table) into Two groups (5 mice/group): Control and IMM0306. For detail, mice were treated with Control (human IgG1 control, 2.5mg/kg, i.v. Day2, 4, 6, 9, 11 and 13), IMM0306 (2.5mg/kg, i.v., Day2, 4, 6, 9, 11 and 13) respectively.

Cell lines culture

Human DLBCL cell lines, OCI-Ly3, U2932, TMD-8, Su-DHL6, Su-DHL10, and DoHH2 were kindly provided by Prof. Feng-Ting Liu (Tianjin Medical University Cancer Institute and Hospital, Tianjin, China), while murine DLBCL cell line A20, myeloma cell line RPMI-8226, human macrophage/monocyte cell line THP-1 cells, and 293T cell line were purchased from ATCC (Manassas, VA, USA). All the tumor cell lines and THP-1 cells were cultured in RPMI 1640 supplemented with 10–20% fetal bovine serum and 1% pen/strep at 37 °C in a humidified incubator with 5% CO₂, while the 293T cell line was cultured in DMEM supplemented with 10% fetal bovine serum and 1% pen/strep at 37 °C in a humidified incubator at 5% CO₂. Before culture, all the cell lines were validated via short tandem repeat analysis and tested for mycoplasma contamination.

Public databases and bioinformatics

We collected gene expression data of 1663 DLBCL patients (693 ABC-DLBCL and 970 GCB-DLBCL) from 4 GEO databases (GSE10846 ³, GSE31312 ⁴, GSE87371⁵, and GSE117556 ⁶), and empirical Bayes ⁷ was used to adjust batch effect, inSilicoMerging⁸ was used to merge the databases, Limma was used to screen DEGs⁹, R package clusterProfiler¹⁰ was used to enrichment analysis of DEGs in KEGG pathway. R (version 4.0.5) was used for statistical computing and graphics.

Plasmid construction, virus production, and transduction

To construct IL-16 knockdown lentiviral vectors, the pLKO.1-Puro plasmid (8453, Addgene, Cambridge, MA, USA) was used. The shRNA-targeting human IL-16 (NM_004513.6) were 5'-GCCAGCCTGGTTTCGCCAAAG-3' for shRNA-#1; 5'-GGAGGAAGGTGCTGGTCTTGG-3' for shRNA-#2; 5'-GGGCCTCACACGGTTTGAAGC-3' for shRNA-#3; and 5'-TTCTCCGAACGTGTCACGT-3' for scrambled RNA.

Further, the pLVX-Puro plasmid (632164, ClonTech, Palo Alto, CA, USA) was used to construct the overexpression lentiviral vectors, human full-length IL-16 (NM_004513.6), human mature IL-16 (truncated human IL-16^{Δ511-631aa} (NM_004513.6)), and murine mature IL-16 (truncated murine IL-16^{Δ507-624aa} (NM_001360089.1)).

To produce lentiviruses in 293T cells, lentiviral vectors with the HIV packaging mix were transfected according to the manufacturer's protocol (LT001, GeneCopoeia Inc., Rockville, MD, USA). Supernatant samples were then harvested after 48 h following centrifugation

at 1,500 g, and incubated with the Lenti-X concentrator (631231, Clonetechnology, Palo Alto, CA, USA). Thereafter, lentiviruses were concentrated according to the manufacturer's instructions, aliquoted and frozen. The target cells were then transduced for 24 h by the lentiviruses using 5–10 µg/ml polybrene, after which the medium was replaced with a fresh complete medium. Then to select stably transduced cells, at 3–4 days intervals, the old medium was replaced with the fresh complete medium containing 1 µg/ml puromycin until drug-resistant colonies were obtained.

Immunohistochemistry (IHC), Immunohistochemical fluorescence (IHF) and multi-immunofluorescence staining(mIHC)

Tissue samples derived from the mouse model were formalin-fixed, paraffin-embedded, and sectioned (4-µm thickness). The tissue slides or tissue microarrays were deparaffinized in xylene and rehydrated using graded ethanol followed by water before staining. Sections were then treated with a buffer as indicated for antigen retrieval in accordance with the instructions corresponding to the primary antibodies and with 3% H₂O₂ for the inactivation of endogenous peroxidase.

To perform IHC, after blocking for 30 min, sections were incubated with primary antibodies overnight at 4 °C. After washing, the sections were stained with a secondary antibody for 30 min at room temperature. Specifically, diaminobenzidine was used as a chromogen substrate, while hematoxylin was used for nuclear counterstaining. Finally, the sections were mounted with nail oil and viewed via microscopy.

Further, to realize IHF, after blocking for 30 min, tissue sections were incubated with primary antibodies overnight at 4 °C, and after washing, they were stained with a secondary antibody for 30 min at room temperature. Thereafter, they were rewashed and stained with the fluorophore-conjugated tyramide signal amplification reagent (G1226, Servicebio, Wuhan, China) for 10 min at room temperature. Then to perform multiple staining, a microwave oven was used to unmask the slices using 10 mM sodium citrate buffer (pH = 6.0) for 10 min, which thereafter, were incubated using another primary antibody, and the above procedure was repeated. Additionally, when it was necessary to realize multiplex plate staining or when only a single test was necessary, the sections were mounted in ProLong Gold anti-fade reagent with DAPI (P36941, Invitrogen, Carlsbad, CA, USA), and viewed via fluorescent microscopy.

The expression intensity and spatial distribution of CD20, CD3, CD68, IL-16 in tumor tissues and lymph node were labeled using mIHC with the Opal 7-color Manual IHC Kit (NEL801001KT, PerkinElmer) and VECTASHIELD® HardSet Antifade Mounting Medium (H-1400, Vector Labs) according to the manufacturer's protocol. Briefly, after the incubating with indicated primary antibodies and secondary antibody as IHC, the tissue sections were stained with Opal 7-color Manual IHC Kit and remove the antibodies through microwaves. Repeat the above steps for another antibody, and mounted as IHF. The Fully automated quantitative pathology imaging system (Vectra Polaris, PerkinElmer) was used

to collect the data and TissueFAXS viewer (TissueGnostics GmbH) was used to analyse data.

RNA extraction, RT-PCR, and q-RT-PCR

RNA was extracted from the cells using Trizol reagent (15596018, Invitrogen, Carlsbad, CA, USA). The RNA pellets thus obtained were then resuspended in 20 μ l of DNase- and RNase-free water, and Reverse Transcriptase-Polymerase Chain Reaction (RT-PCR) (RR036Q, Takara, Tokyo, Japan) as well as Real-time RT-PCR (q-RT-PCR) (RR430S, Takara, Tokyo, Japan) were performed on the extracted RNA according to the manufacturer's instructions. The primer sequences for IL-16 were 5'-GACACAGGGTTCTCGCTCAA-3' (forward) and 5'-GTCTTCCTTGGCTTCCGTGA-3' (reverse), while those for β -actin were 5'-ACACCTTCTACAATGAGCTG-3' (forward) and 5'-CATGATGGAGTTGAAGGTAG-3' (reverse).

RNA-seq analysis

RNA samples (three biological replicates) were collected from U-2932 and TMD-8 cell lines with or without Pre-IL-16 knock-down. Thereafter, total RNA was extracted and used for RNA-seq analysis. The cDNA library was constructed and sequenced by Beijing Genomics Institute (BGI, Beijing, China) using the BGISEQ-500 platform, and high-quality reads were aligned to the human reference genome, GRCh38, using Bowtie2. Further, the expression levels of the different genes were normalized to fragments per kilobase of exon model per million mapped reads using RNA-seq via Expectation-

Maximization. Significant differentially expressed genes (DEGs) with absolute log₂ ratio values ≥ 1 and the combination of Q values ≤ 0.05 were then confirmed using BGI Bioinformatics Service. RNA-seq data are available at SRA under BioProject ID: PRJNA786965 (<https://www.ncbi.nlm.nih.gov/sra/PRJNA786965>).

Cell viability assay

Cell viability was determined using the Cell Counting Kit-8 (CCK-8) (HY-K0301, MCE, Shanghai, China). Specifically, 10 μ l of the CCK-8 reagent was added to the cell culture medium in 96-well plates for 2h, after which absorbance was measured at 450 nm using a microplate reader.

Flow cytometry

To determine the cell surface expression of the indicated protein, cells were incubated with TruStain FcX™ PLUS or Human TruStain FcX™ antibody (156603, 422301, Biolegend, San Diego, CA, USA) to block Fc receptors for 5min on ice. Thereafter, cells were stained with indicated antibodies, or relevant isotype controls on ice for 15 min in the dark, after which the cells were washed using PBS supplemented with 2% FBS and subjected to flow cytometry.

Further, to determine the percentage of apoptotic cells, DLBCL cells were stained with 7-AAD and Annexin V (640930, Biolegend, San Diego, CA, USA) according to the manufacturer's protocol, and thereafter subjected to flow cytometry. Further, to determine

caspase-3 and caspase-7 activation, DLBCL cells were stained with SYTOX™ AADvanced™ and CellEvent™ caspase 3/7 green detection reagent according to the manufacturer's protocol (C10427 Invitrogen, Carlsbad, CA, USA) and analyzed via flow cytometry.

Western blotting

Protein samples were extracted from tumor cell lines and tissues using CellLytic™ M cell Lysis Reagent (C2978, Sigma-Aldrich, St. Louis, MO, USA) and Tissue Extraction Reagent I (FNN0071, Invitrogen, Carlsbad, CA, USA), which is provided alongside protease and phosphatase inhibitor cocktails (78446, Invitrogen, Carlsbad, CA, USA). The extracted protein samples were loaded onto 4–12% SurePAGE™ Bis-Tris 10x8 gels (M00654, GenScript, Piscataway, NJ, USA) and within 5–10 min, transferred onto a 0.45- μ m PVDF membrane (IPVH00010, Millipore, Billerica, MA, USA) using the eBlot™ L1 wet protein transfer system (L00686C, GenScript, Piscataway, NJ, USA). Thereafter, the PVDF membrane was blocked using the blocking buffer (5% polyvinyl pyrrolidone PVP, 5% fetal calf serum, and 0.1% sodium azide in tris-buffered solution [TBS] containing 0.2% Tween-20 [TBST]) for 60 min and then incubated with primary antibodies overnight at 4 °C. Bound antibodies were then detected via incubation using horseradish peroxidase-conjugated secondary antibodies in TBST.

Cytokine array and enzyme-linked immunosorbent assay (ELISA)

Serum samples from a patient with ABC-DLBCL collected at indicated time points were used for cytokine array analyses with human inflammation antibody array (40 Targets) (ab134003, Abcam, Cambridge, MA, USA) according to the manufacturer's instruction.

To determine serum IL-16 levels, ELISA was performed using the human IL-16 ELISA Kit (EH259RBX10, Invitrogen, Carlsbad, CA, USA) and murine IL-16 ELISA Kit (SEA062, Cloud-Clone Corp., Wuhan, China) following the manufacturer's instruction. In brief, serum samples were collected from DLBCL patients or the culture medium of DLBCL cell lines at indicated time points and subsequently subjected to ELISA in accordance with the manufacturer's protocol. Absorbances at 450 nm were then measured using a microplate reader.

Tumor cells isolation from tumor tissues

Tumor tissues were excised and digested post-mortem using a cocktail of 1 mg/mL collagenase type II (A004174, Sangon, Shanghai, China) and 0.02 mg/mL DNAase (10104159001, Sigma-Aldrich, St. Louis, MO, USA). After digestion at 37°C for 30 minutes under continuous rotation (1,000rpm). Red Blood Cell Lysis Solution (130-094-183, Miltenyi Biotec, Shanghai, China) was to remove erythrocytes. Cells were passed through a 70-mm filter twice and then analyzed.

Isolation of Human Peripheral Blood Leucocyte (PBLs) and Human Blood Monocytes

Whole Blood from healthy donors was collected in Venous Blood Collection Tubes containing EDTA and stored immediately at 4 °C after collection. Red Blood Cell Lysis Solution (130-094-183, Miltenyi Biotec, Shanghai, China) was added to the whole Blood and incubated for 10 minutes at room temperature, and then centrifuge at 300xg for 10 minutes, and aspirate supernatant completely. Resuspend the cell pellet (PBLs) in PBS with 2% FBS and passed through a 70-mm filter twice for further analysis.

Monocytes were isolated by Dynabeads® Untouched™ Human Monocytes kit (11350D, Invitrogen, Carlsbad, CA, USA) according to the manufacturer's protocol. Briefly, 5×10^7 PBLs were mixed with blocking reagent and antibody mix, and incubated for 20min at 4 °C. Wash the cells and mixed them with pre-washed Dynabeads, and incubate them for 15min at 4 °C. Resuspend the bead-bound cells thoroughly and placed the tube in the magnet for 2min. Transfer the supernatant containing the untouched human monocytes, to a new larger tube. Monocytes were used for further analysis.

Antibody-dependent cellular phagocytosis (ADCP)

Effector cells (THP-1 cells, a human macrophage/monocyte cell line) and DLBCL cells were labeled with CellTrace™ Violet and CellTrace™ CFSE (C34554, C34557, Invitrogen, Carlsbad, CA, USA) respectively according to the manufacturer's protocol. Aliquot labeled DLBCL cells and effector cells at the indicated ratio in a 96-well round-bottom plate, and add the IMM0306 (ImmuneOnco, Shanghai, China) or IgG1 mAb (BE0297, Bio X Cell, Lebanon, NH, USA) in the plate. Incubate the plate for 30min at 37°C in a 5% CO₂

incubator. Wash the cells with PBS supplemented with 2% FBS and proceed to analysis on a flow cytometer. The double-stained cells were phagocytosed tumor cells.

In Vitro Cell Migration Assay

Cells were washed in PBS, centrifuged at 300xg for 5 minutes, and resuspended in 0.1% BSA RPMI-1640 medium. Transwell chambers (5µm core, 3421, Corning, NY, USA) were prepared to fill with 500 µL of indicated CM in the lower chamber. 100 µL 5x10⁵ cells were plated in the upper insert of each Transwell chamber and incubated at 37°C for 1h. Relative cell numbers of the lower chamber were determined using the Cell Counting Kit-8 (CCK-8) (HY-K0301, MCE, Shanghai, China) and the absorbance was measured at 450 nm using a microplate reader. Rate of chemotaxis (%)=(OD_{Lower chamber}-OD_{Background}/OD_{Upper chamber}-OD_{Background})x100.

Statistical analysis

Data were presented as either mean or median ± SEM or SD, and statistical significance was determined by performing the two-tailed Student's paired or unpaired t-test, one-way or two-way ANOVA, and the Chi-square test. Further, Pearson product-moment correlation analysis was employed to analyze the linearity of the correlation between the two groups. To perform categorical analysis, i.e., divide patients into two cohorts based on serum IL-16 levels, the X-tile statistical package was used¹¹. Outcomes, which were measured from the date of diagnosis to the date of adverse event occurrence or last follow-up, included overall survival (OS) and patient free survival (PFS) rates, and Log-rank

(Mantel-Cox) test and Cox regression were used to evaluate the relationship between the clinical features or gene expressions and OS or PFS. Sample sizes were determined according to pilot studies and based on previous experimental experiences. Experiments were biologically replicated three times in the cell-level study. For *in vitro* studies, the sample size in each group was at least 3, for *in vivo* studies, the sample size in each group was at least 4, and for the studies of tumor therapeutic outcomes, the sample size in each group was at least 5. For all the different statistical analyses, $P < 0.05$ were considered significant, * $P < 0.05$, ** $P < 0.01$; *** $P < 0.001$, and **** $P < 0.0001$. Data analyses were performed using Prism software (Version of 9, GRAPH PAD Software Inc., San Diego, CA, USA) and SPSS software (Version of 24, IBM, Armonk, NY, USA).

References

1. Moreno SG. Depleting Macrophages In Vivo with Clodronate-Liposomes. *Methods Mol Biol.* 2018;1784:259-262.
2. Yu J, Li S, Chen D, et al. IMM0306, a fusion protein of CD20 mAb with the CD47 binding domain of SIRPalpha, exerts excellent cancer killing efficacy by activating both macrophages and NK cells via blockade of CD47-SIRPalpha interaction and FcγR engagement by simultaneously binding to CD47 and CD20 of B cells. *Leukemia.* 2023;37(3):695-698.
3. Lenz G, Wright G, Dave SS, et al. Stromal gene signatures in large-B-cell lymphomas. *N Engl J Med.* 2008;359(22):2313-2323.
4. Xu-Monette ZY, Moller MB, Tzankov A, et al. MDM2 phenotypic and genotypic profiling, respective to TP53 genetic status, in diffuse large B-cell lymphoma patients treated with rituximab-CHOP immunochemotherapy: a report from the International DLBCL Rituximab-CHOP Consortium Program. *Blood.* 2013;122(15):2630-2640.
5. Dubois S, Vially PJ, Bohers E, et al. Biological and Clinical Relevance of Associated Genomic Alterations in MYD88 L265P and non-L265P-Mutated Diffuse Large B-Cell Lymphoma: Analysis of 361 Cases. *Clin Cancer Res.* 2017;23(9):2232-2244.

6. Sha C, Barrans S, Cucco F, et al. Molecular High-Grade B-Cell Lymphoma: Defining a Poor-Risk Group That Requires Different Approaches to Therapy. *J Clin Oncol*. 2019;37(3):202-212.
7. Johnson WE, Li C, Rabinovic A. Adjusting batch effects in microarray expression data using empirical Bayes methods. *Biostatistics*. 2007;8(1):118-127.
8. Taminau J, Meganck S, Lazar C, et al. Unlocking the potential of publicly available microarray data using inSilicoDb and inSilicoMerging R/Bioconductor packages. *BMC Bioinformatics*. 2012;13:335.
9. Ritchie ME, Phipson B, Wu D, et al. limma powers differential expression analyses for RNA-sequencing and microarray studies. *Nucleic Acids Res*. 2015;43(7):e47.
10. Yu G, Wang LG, Han Y, He QY. clusterProfiler: an R package for comparing biological themes among gene clusters. *OMICS*. 2012;16(5):284-287.
11. Camp RL, Dolled-Filhart M, Rimm DL. X-tile: a new bio-informatics tool for biomarker assessment and outcome-based cut-point optimization. *Clin Cancer Res*. 2004;10(21):7252-7259.

Supplementray tables

Supplementray Table 1. Key reagent or resources

Reagent or Resource	Source	Identifier
Antibodies and recombinant protein		
Rabbit monoclonal anti-IL-16 [EPR19988]	Abcam	Cat#: ab207181
Mouse IL-16 Biotinylated Antibody	R&D	Cat#: BAF1727
Caspase-3 Antibody	CST	Cat#: 9662
Cleaved Caspase-3 (Asp175) (5A1E) Rabbit mAb	CST	Cat#: 9661
β -Actin (8H10D10) Mouse mAb	CST	Cat#: 3700
Anti-rabbit IgG, HRP-linked Antibody	CST	Cat#: 7074
Anti-mouse IgG, HRP-linked Antibody	CST	Cat#: 7076
F4/80 (D2S9R) XP® Rabbit mAb	CST	Cat#: 70076
CD3 ϵ (E4T1B) XP® Rabbit mAb	CST	Cat#: 78588
CD3 ϵ (D7A6E™) XP® Rabbit mAb	CST	Cat#: 85061
CD4 (D7D2Z) Rabbit mAb	CST	Cat#: 25229
CD8 α (D4W2Z) XP® Rabbit mAb	CST	Cat#: 98941
CD11c (D1V9Y) Rabbit mAb	CST	Cat#: 3850
Anti-MS4A1 antibody produced in rabbit	Sigma	Cat#: HPA014341
CD68 (E3O7V) Rabbit mAb	CST	Cat#: 97778
FoxP3 (D6O8R) Rabbit mAb	CST	Cat#: 12653
Granzyme B (E5V2L) Rabbit mAb	CST	Cat#: 3850
Ly-6G (E6Z1T) Rabbit mAb	CST	Cat#: 87048
T-bet/TBX21 (E4I2K) Rabbit mAb	CST	Cat#: 97135

Siglec-H Antibody (23M15C8)	R&D	Cat#: NBP2-27062
CD31 (PECAM-1) (D8V9E) XP® Rabbit mAb	CST	Cat#: 77699
CD86 (E5W6H) Rabbit mAb	CST	Cat#: 19589
Anti-CD163 antibody [EPR19518]	Abcam	Cat#: ab182422
Anti-IL-6 antibody [1.2-2B11-2G10]	Abcam	Cat#: ab9324
Anti-IL-10 antibody [JES5-2A5]	Abcam	Cat#: ab189392
Goat anti-Rabbit IgG (H+L) Secondary Antibody, HRP	invitrogen	Cat#: 31460
Goat anti-Mouse IgG (H+L) Secondary Antibody, HRP	invitrogen	Cat#: 31430
Pacific Blue™ anti-human CD8 Antibody	Biolegend	Cat#: 344717
FITC Mouse Anti-Human CD4	BD	Cat#: 555346
APC anti-human CD14 Antibody	Biolegend	Cat#: 325607
PE/Cyanine7 anti-human CD3	Biolegend	Cat#: 980010
PE anti-human CD9 Antibody	Biolegend	Cat#: 312105
PE anti-human CD4 Antibody	Biolegend	Cat#: 300508
PE anti-human CD138 (Syndecan-1) Antibody	Biolegend	Cat#: 352305
PE anti-human CD19 Antibody	Biolegend	Cat#: 302254
APC/Cyanine7 anti-human CD11b Antibody	Biolegend	Cat#: 301341
Human TruStain FcX™ (Fc Receptor Blocking Solution)	Biolegend	Cat#: 422301
Recombinant human IL-16 protein (Active) (ab256039)	Abcam	Cat#: ab259416
InVivoMAb human IgG1 isotype control	Bio X Cell	Cat#: BE0297

Chemicals

Vincristine sulfate	MCE	Cat#: HY-N0488
Doxorubicin hydrochloride	MCE	Cat#: HY-15142
4-Hydroperoxy Cyclophosphamide	Santa Cruz	Cat#: 39800-16-3
PAC-1	MCE	Cat#: HY-13523
Matrigel matrix high protein	BD	Cat#: 354248
Streptavidin (HRP)	Abcam	Cat#: ab7403
Puromycin Dihydrochloride	MCE	Cat#: HY-B1743A
Polybrene	Santa Cruz	Cat#: sc-134220
Clodronate Liposomes	Yeasen	Cat#: 40337ES10
APC Annexin V	Biolegend	Cat#: 640941
7-AAD	BD	Cat#: 559925
DAPI Solution	BD	Cat#: 564907

Critical commercial assays

Lenti-Pac HIV Expression Packaging Kit	GeneCopoeia	Cat#: LT001
TSA Plus multi-fluorophore detection kit	Servicebio	Cat#: G1226
Human IL-16 ELISA Kit	invitrogen	Cat#: EH259RB
ELISA Kit for Interleukin 16 (IL16)	Cloud-Clone Corp.	Cat#: SEA062Mu
CellEvent™ Caspase 3/7 Green Ready Flow™ Reagent	invitrogen	Cat#: R37167

Human Inflammation Antibody Array (40 Targets)	Abcam	Cat#: ab134003
Dynabeads® Untouched™ Human Monocytes kit	invitrogen	Cat#: 11350D
CellTrace™ CFSE Cell Proliferation Kit, for flow cytometry	invitrogen	Cat#: C34554
CellTrace™ Violet Cell Proliferation Kit	invitrogen	Cat#: C34557

Supplementray Table 2. Baseline clinical characteristics of *de novo* patients with ABC-DLBCL or GCB DLBCL

Characteristic	ABC-DLBCL (n=45)		GCB-DLBCL (n=39)	
	n	(% of total)	n	(% of total)
Age, y				
≤60	23	51.11	27	69.23
>60	22	48.89	12	30.77
Sex				
Male	26	57.78	22	56.41
Female	19	42.22	17	43.59
ECOG PS				
≤1	40	88.89	23	58.97
>1	5	11.11	16	41.03
Serum LDH level				
Normal	25	55.56	23	58.97
Elevated	20	44.44	16	41.03
Serum β2M level				

Normal	19	42.22	23	58.97
Elevated	19	42.22	9	23.08
Unknown	7	15.56	7	17.95
Ann Arbor stage				0.00
I/II	14	31.11	22	56.41
III/IV	31	68.89	17	43.59
B symptoms				
Absent	30	66.67	28	71.79
Present	15	33.33	11	28.21
IPI				
<2	19	42.22	22	56.41
≥2	26	57.78	17	43.59
No. of identified extranodal sites				
<2	31	68.89	29	74.36
≥2	14	31.11	10	25.64
DEL				
Absent	33	73.33	32	82.05
Present	12	26.67	7	17.95
Treatment				
R-CHOP	23	51.11	18	46.15
R-EDOCH	20	44.44	21	53.85
R-miniCHOP	2	4.44	0	0.00
Therapeutic response				
CR	33	73.33	35	89.74

PR	7	15.56	1	2.56
SD+PD	4	8.89	1	2.56
Unknown	1	2.22	2	5.13

ECOG PS, Eastern Cooperative Oncology Group performance status; IPI, International Prognostic Index; LDH, lactate dehydrogenase; DEL, double expression lymphoma (MYC and BCL2 protein expression).

Supplementray figures

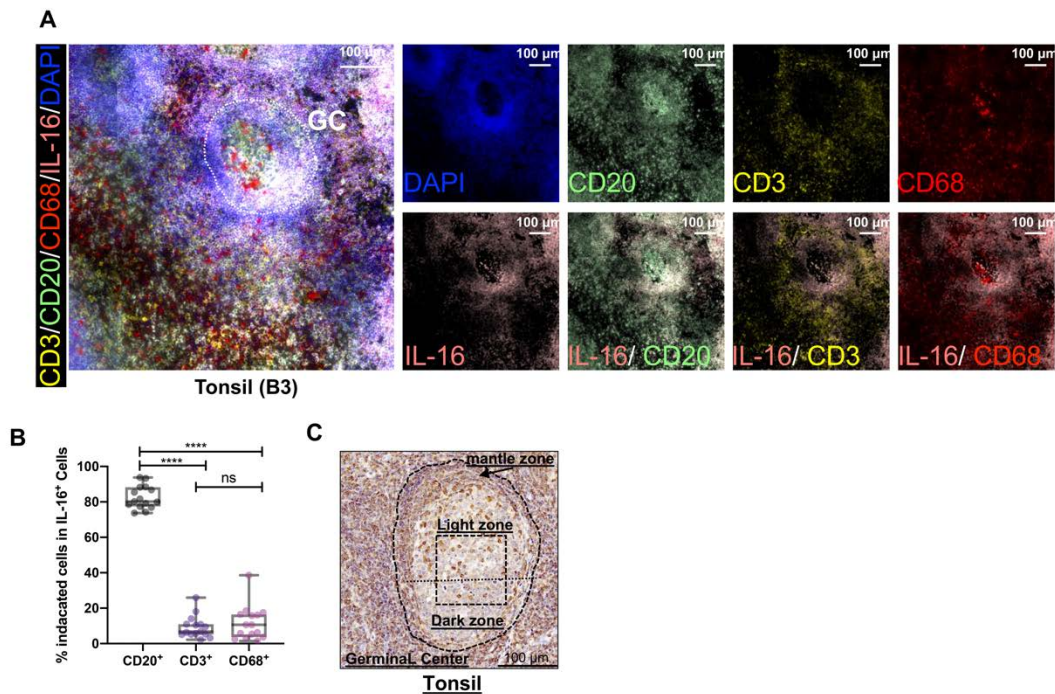


fig. S1. (A) Representative mIHC images for IL-16 protein expression (pink pseudocolor) in tonsil specimens. CD20 (B cells, green pseudocolor), CD3 (T cells, yellow pseudocolor), CD68 (macrophages, red pseudocolor), and DAPI nuclear stain (blue pseudocolor) included to discern tissue landscape. Scale bars apply across each row. (B) Proportion of IL-16-positive cells in different types of immune cells. $n=15$. (C) Representative IHC images for IL-16 protein expression in tonsil specimens. Data shown are mean \pm SD. p values are based on unpaired t-test. ns=non-significant; * $p < 0.05$, ** $p < 0.01$, *** $p < 0.001$, **** $p < 0.0001$.

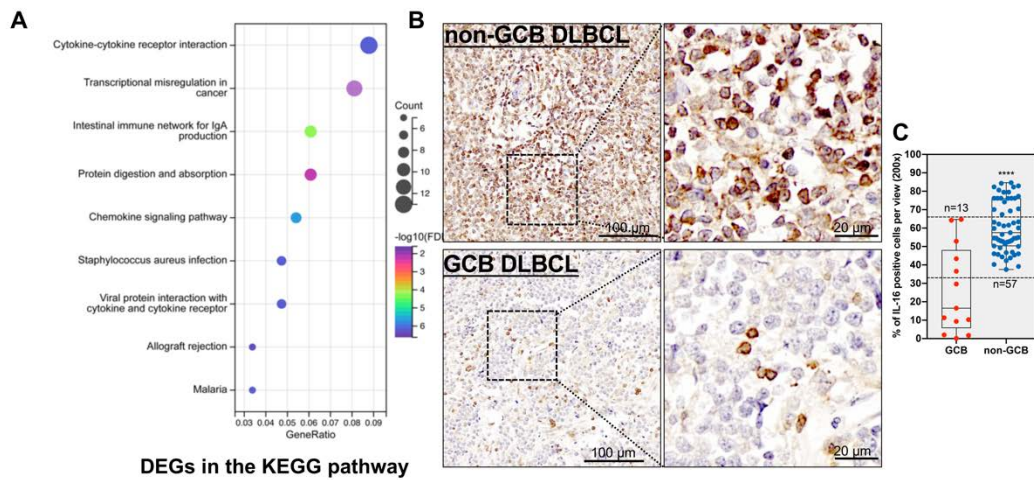


fig. S2. (A) The bubble diagram indicates the enrichment analysis of DEGs in KEGG pathway by clusterProfiler. (B-C) Representative IHC and quantification for IL-16 protein expression in DLBCL tissues. Boxed regions are magnified right. Scale bars apply across each row. The difference of IL-16 positive cells between GCB DLBCL (n=13) and non-GCB DLBCL (n=57) is analyzed. Data shown are mean \pm SD. p values are based on unpaired t-test. ns=non-significant; *p < 0.05, **p < 0.01, ***p < 0.001, ****p < 0.0001.

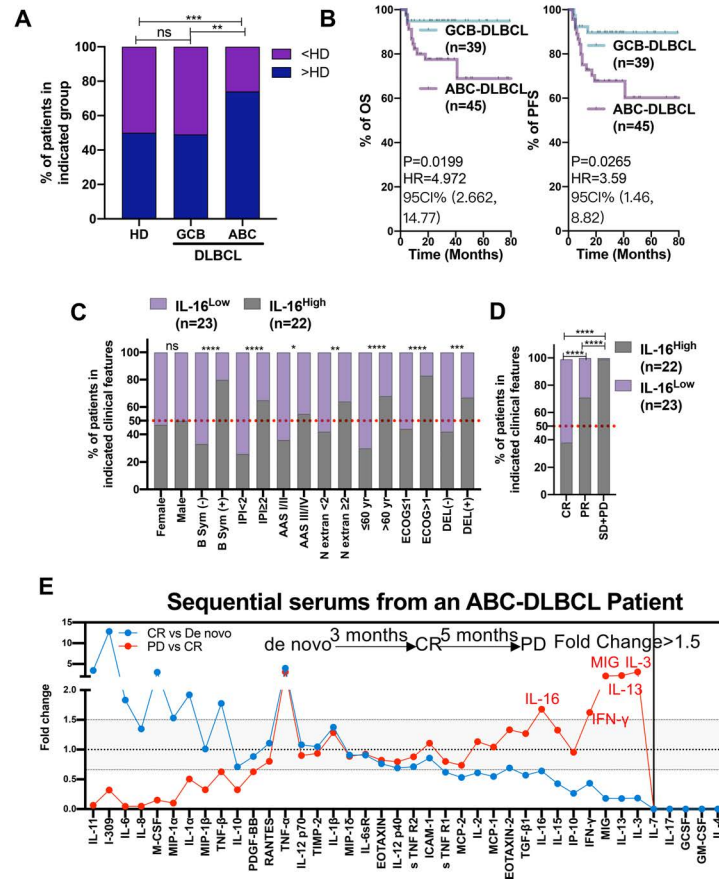


fig. S3. (A) Detection of the levels of IL-16 in serum from DLBCL patients (39 GCB-DLBCL and 45 ABC-DLBCL) and health donors (n=10) by ELISA. Proportion of patients in indicated group (the mean of IL-16 levels in the serum of healthy donors was used as a basis for grouping). (B) OS and PFS of DLBCL patients based COO. (C) The differences in serum IL-16 of ABC-DLBCL patients between indicated clinical features are analyzed. (D) The differences in serum IL-16 of ABC-DLBCL patients between the response to treatment are analyzed. (E) Determination of the relative differences (fold change) of 40 cytokines in sequential serums from an ABC-DLBCL patient between different time points (CR vs de novo and PD vs CR) by human inflammation antibody

array. Red symbols are cytokines that are markedly varied in the two comparisons (> 1.5 fold change). p values are based Pearson correlation, Chi-square test, and Cox regression. ns=non-significant; * $p < 0.05$, ** $p < 0.01$, *** $p < 0.001$, **** $p < 0.0001$.

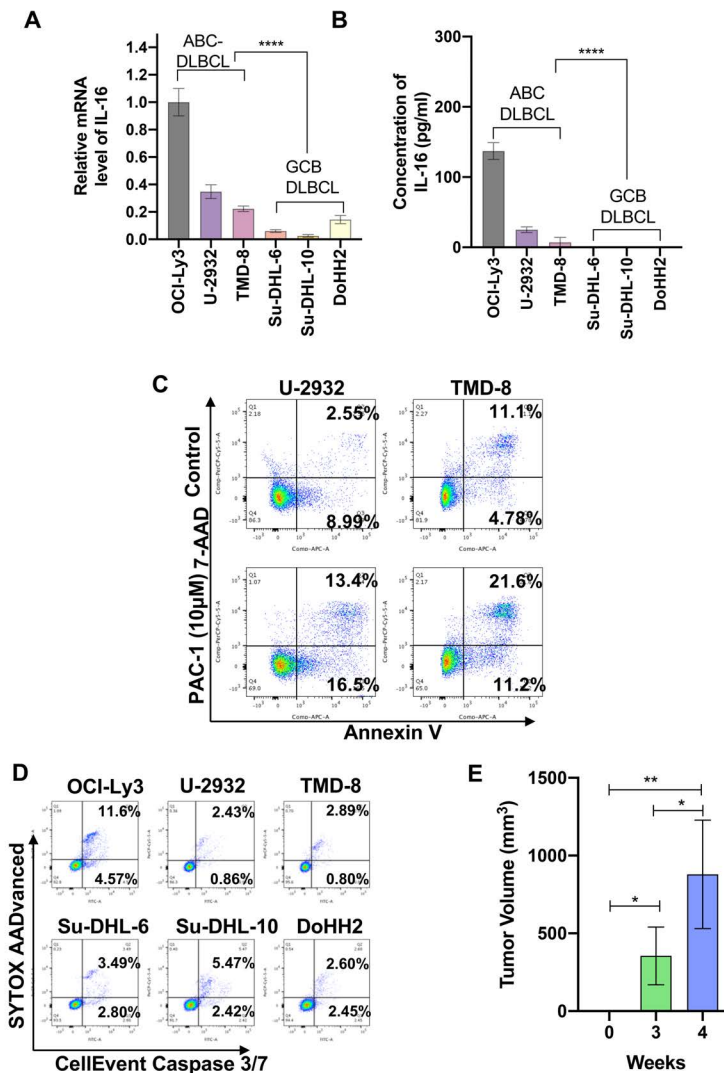


fig. S4. (A) Secretion levels of IL-16 in the culture medium of DLBCL cell lines (OCI-Ly3, TMD-8, U-2932, Su-DHL-6, Su-DHL-10, and DoHH2) (5×10^5 cells/ml, 24h) are quantified by ELISA. (B) IL-16 transcript levels in DLBCL cell lines (OCI-Ly3, TMD-8, U-2932, Su-DHL-6, Su-DHL-10, and DoHH2) are quantified by qPCR and normalized to

the expression in OCI-Ly3 cells. β -Actin serves as a reference gene. (C) ABC-DLBCL cell lines (U-2932 and TMD-8) are treated with 10 μ M PAC-1 or DMSO for 24 h, and percentages of apoptosis are determined by flow cytometry (Annexin V and 7-AAD double staining) and analyzed by Flowjo. (D) Caspase-3/7 activation of untreated DLBCL cell lines (OCI-Ly3, U-2932, TMD-8, Su-DHL-6, Su-DHL-10, and DoHH2) is determined by flow cytometry (CellEvent Caspase-3/7 and SYTOX AADvanced double staining) and analyzed by Flowjo. (E) The BALB/c mice were inoculated subcutaneously with A20 cells (n=4/group), the serum was collected at different time points (week0, week3 and week4), and the tumor tissues were collected at different time points (week3 and week4). Data shown are mean \pm SD. p values are based on one-way ANOVA and unpaired t-test. ns=non-significant; *p < 0.05, **p < 0.01, ***p < 0.001, ****p < 0.0001.

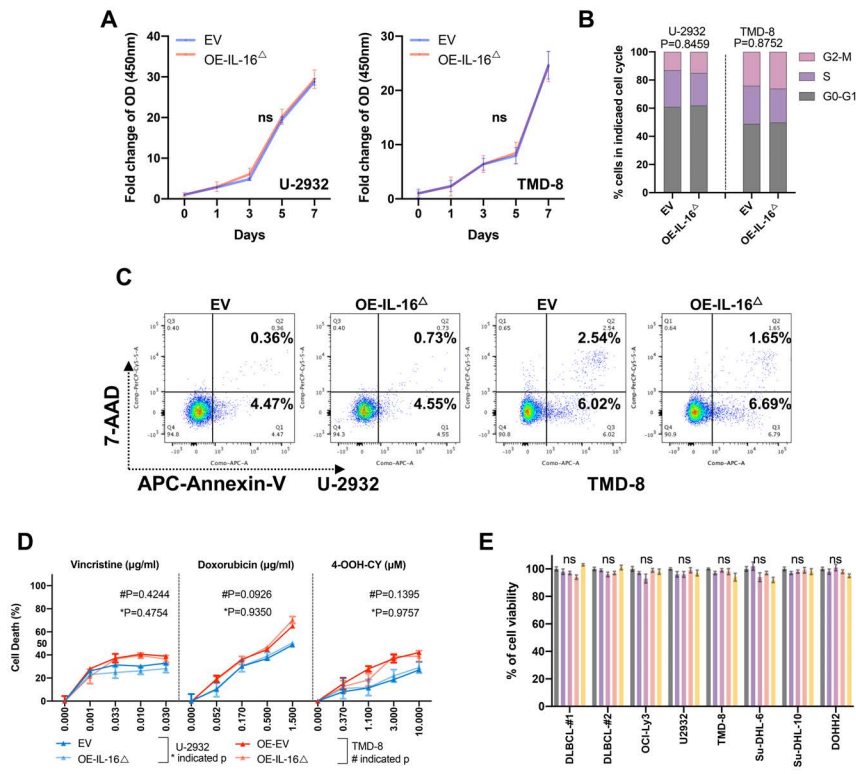


fig. S5. (A-D) U-2932 and TMD-8 with stable overexpression of IL-16 $\Delta^{511-631aa}$ (labeled with IL-16 Δ) or EV are cultured *in vitro*. **(A)** OD of cells mixed with CCK-8 was determined at indicated time points. Fold change=(OD_{Day-n}-OD_{background})/ (OD_{Day-0}-OD_{background}). **(B)** The cell cycle is determined by flow cytometry (DAPI staining) and analyzed by Flowjo. **(C)** Apoptosis is determined by flow cytometry (Annexin V-APC and 7-AAD double staining) and analyzed by Flowjo. **(D)** Cells are treated with indicated doses of Vincristine, Doxorubicin, 4-OOH-CY, or DMSO for 24 h, and percentages of cell death are determined by the CCK-8 test. **(E)** Primary cells from 2 DLBCL tissues and DLBCL cell lines (OCI-Ly3, TMD-8, U-2932, Su-DHL-6, Su-DHL-10, and DoHH2) are treated with indicated doses of rh-IL-16 for 24 h, and percentages of cell viability are

determined by the CCK-8 test. Data shown are mean \pm SD. p values are based on the one-way or two-way ANOVA and Chi-square test.

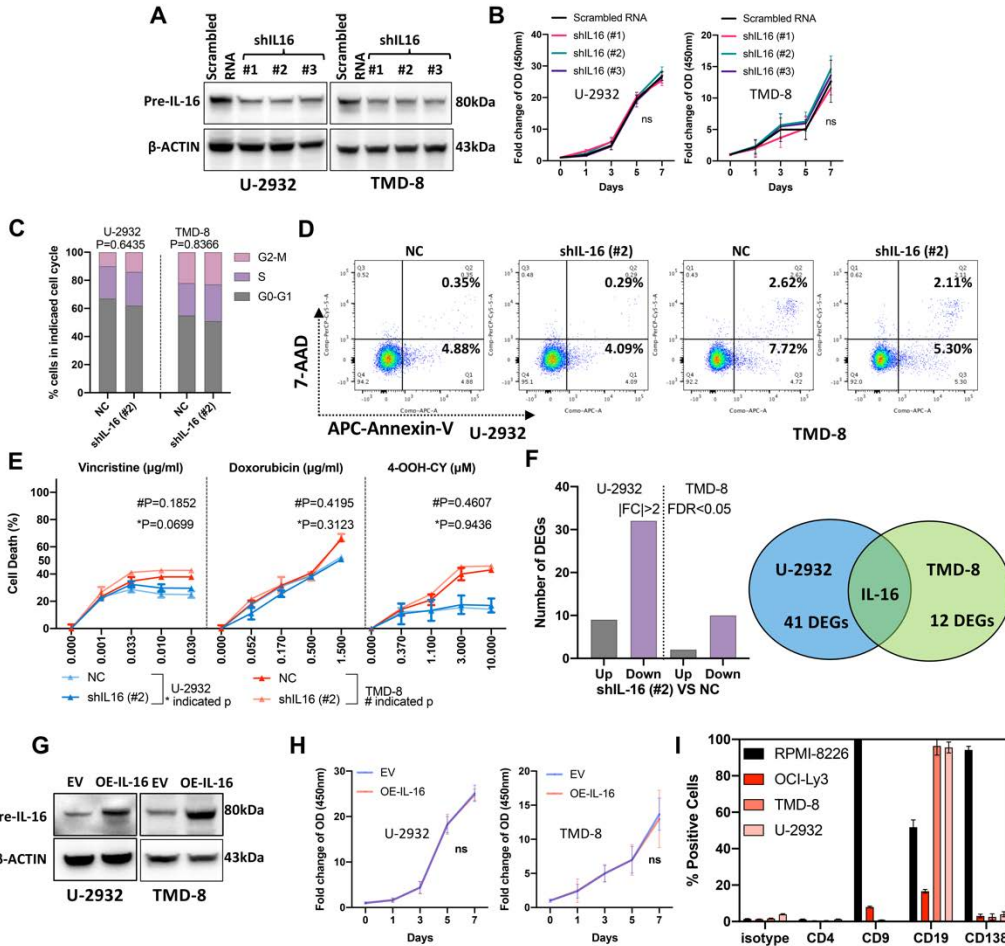


fig. S6. (A) Detection of IL-16 protein expression by western blotting in DLBCL cell lines (U-2932 and TMD-8) with stable Pre-IL-16 expression knockdown (shIL16 #1, #2 and #3) or NC. β -Actin is used as a loading control. NC (Negative Control) indicated scrambled RNA (B-F) U-2932 and TMD-8 cells with stable Pre-IL-16 expression knockdown or NC are cultured *in vitro*. (B) Optical density (OD) of cells mixed with CCK-8 were determined at indicated time points. Fold change=(OD_{Day-n}-OD_{background})/

($OD_{\text{Day-0}} - OD_{\text{background}}$). (C) The cell cycle is determined by flow cytometry (DAPI staining) and analyzed by Flowjo. (D) Apoptosis is determined by flow cytometry (Annexin V-APC and 7-AAD double staining) and analyzed by Flowjo. (E) Cells are treated with indicated doses of Vincristine, Doxorubicin, 4-OOH-CY, or DMSO for 24 h, and percentages of cell death are determined by the CCK-8 test. (F) RNA-seq is used to detect differential expression genes (DEGs). Numbers of genes are upregulated (Up) or downregulated (Down) by Pre-IL-16 expression knockdown ($|FC| > 2$, $FDR < 0.05$). The Venn diagram was shown the overlap between DEGs detected in U-2932 cell lines and TMD-8 cell lines. (G) Detection of IL-16 protein expression by western blotting in DLBCL cell lines (U-2932 and TMD-8) with stable overexpression of Pre-IL-16 or NC. β -Actin is used as a loading control. NC indicated empty vector controls. (H) U-2932 and TMD-8 cells with stable Pre-IL-16 expression overexpression or NC are cultured *in vitro*. Optical density (OD) of cells mixed with CCK-8 were determined at indicated time points. $\text{Fold change} = (OD_{\text{Day-n}} - OD_{\text{background}}) / (OD_{\text{Day-0}} - OD_{\text{background}})$. (I) Determination of CD4, CD9, CD19 and CD138 expression on three ABC-DLBCL cell lines (OCI-Ly3, TMD-8, and U-2932) and myeloma cells (RPMI-8226) by flow cytometry. Cells are stained with anti-CD4, CD9, CD19 and CD138 antibodies (PE) or mouse IgG-PE control isotype respectively. Data shown are mean \pm SD. p values are based on the one-way or two-way ANOVA, Chi-square test, unpaired or paired t-test. ns=non-significant; * $p < 0.05$, ** $p < 0.01$, *** $p < 0.001$, **** $p < 0.0001$.

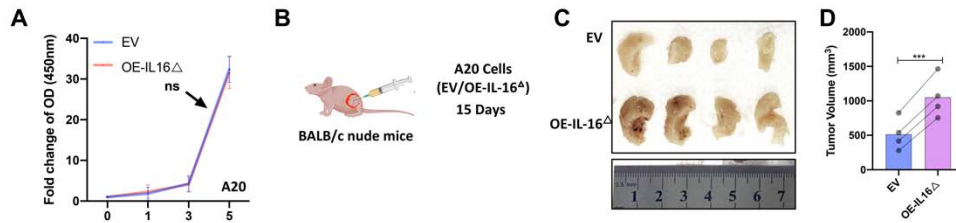


fig. S7. (A) A20 cells with stable overexpression of murine IL-16 $\Delta^{507-624aa}$ or EV are cultured *in vitro* and percentages of cell viability are determined by the CCK-8 test. (B-D) BALB/c nude mice are inoculated with A20 cells with murine IL-16 $\Delta^{507-624aa}$ overexpression or EV respectively for 15 days (n=4/group). A collection of tumors and tumor volumes from mice. Data shown are mean \pm SD. p values are based on the one-way or two-way ANOVA and paired t-test. ns=non-significant; *p < 0.05, **p < 0.01, ***p < 0.001, ****p < 0.0001.

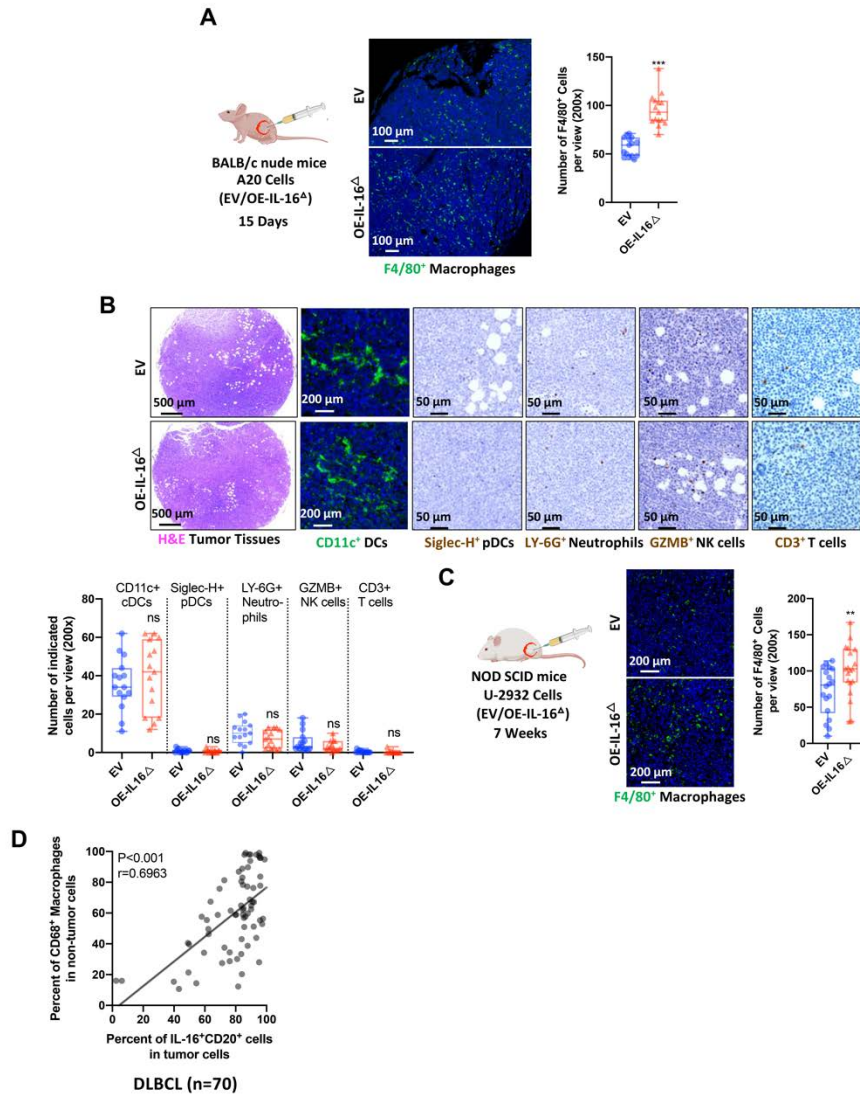


fig. S8. (A) Representative immunostaining and quantification for the F4/80⁺ macrophages in sections of tumor tissues from BALB/c nude mice. The differences in the infiltration of F4/80⁺ macrophages in indicated tumor tissues between different groups (murine IL-16^{Δ507-624aa} overexpression vs EV) are analyzed. (B) Representative stain for H&E in the sections of indicated tumor tissues from BALB/c nude mice. Representative immunostaining and quantification for the indicated immune cells of tumor tissues from BALB/c nude mice. The differences in the infiltration of indicated immune cells in

indicated tumor tissues between different groups (murine IL-16 $\Delta^{507-624aa}$ overexpression vs EV) are analyzed. (C) Representative immunostaining and quantification for the F4/80 $^{+}$ macrophages in sections of tumor tissues from NOD SCID mice. The differences in the infiltration of F4/80 $^{+}$ macrophages in indicated tumor tissues between different groups (IL-16 $\Delta^{511-631aa}$ overexpression vs EV) are analyzed. (D) The correlation between the proportion of IL-16 $^{+}$ CD20 $^{+}$ cells in tumour cells and the proportion of CD68 $^{+}$ macrophages in non-tumour cells as shown in Figure 2D. (n=70). Data shown are mean \pm SD. p values are based on unpaired t-test and Pearson correlation.. ns=non-significant; *p < 0.05, **p < 0.01, ***p < 0.001, ****p < 0.0001.

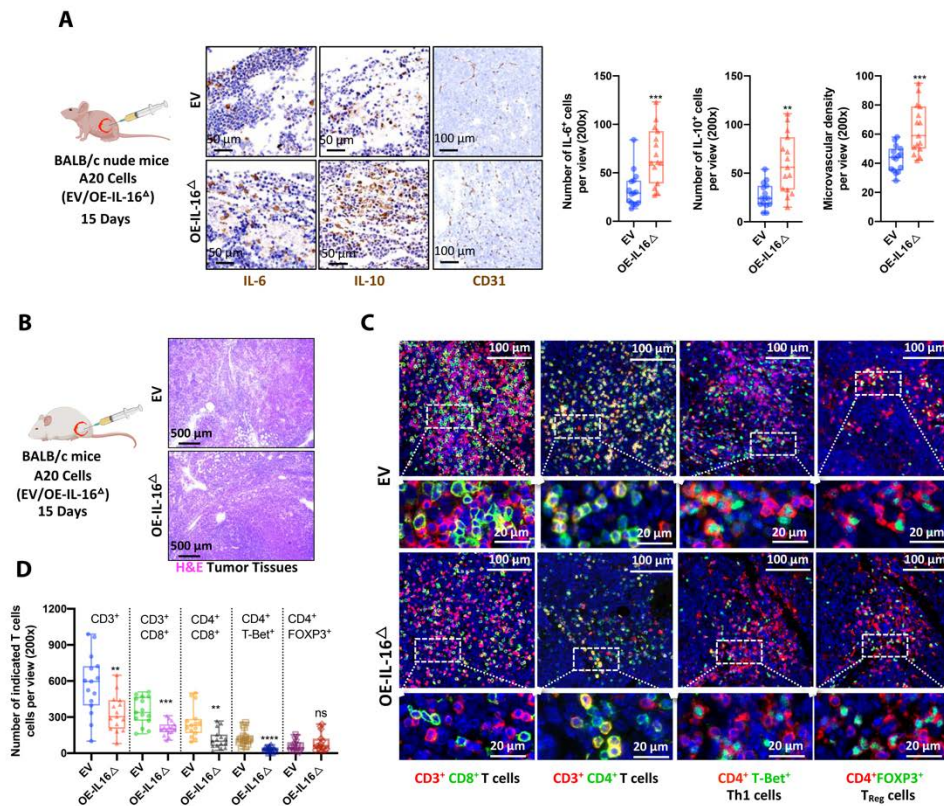


fig. S9. (A) Representative immunostaining and quantification for the cytokines IL-6 and IL-10, and vascular endothelial cells marker CD31 (microvascular density) in the sections of tumor tissues from BALB/c nude mice. The difference in the infiltration of indicated cells in tumor tissues between different groups (murine IL-16 $\Delta^{507-624aa}$ overexpression vs EV) is analyzed. (B) Representative stain for H&E in the sections of indicated tumor tissues from BALB/c mice. (C-D) Representative immunostaining and quantification for CD3 and CD8, CD3 and CD4, CD4 and T-Bet, and CD4 and FOXP3 in the sections of tumor tissues. The difference in the infiltration of indicated cells in tumor tissues between different groups (murine IL-16 $\Delta^{507-624aa}$ overexpression vs EV) is analyzed. Scale bars apply across each row. Data shown are mean \pm SD. p values are based on unpaired t-test. ns=non-significant; *p < 0.05, **p < 0.01, ***p < 0.001, ****p < 0.0001.

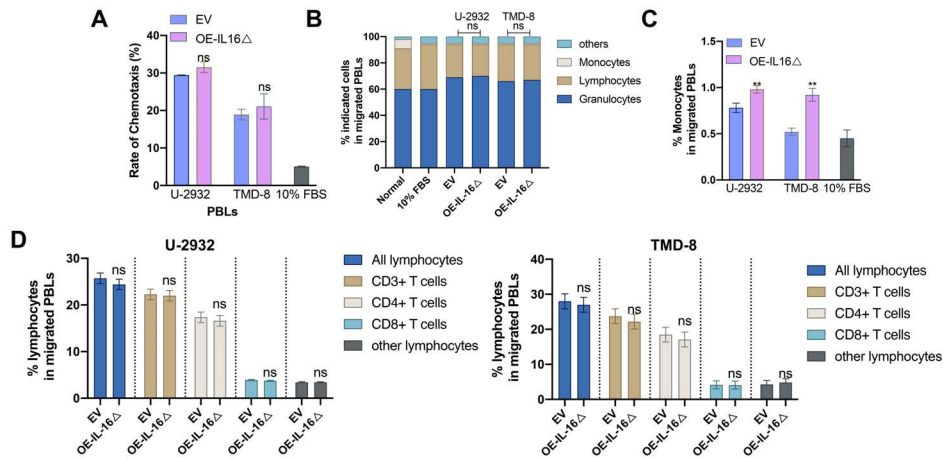


fig. S10. (A) The culture medium of indicated DLBCL cells (U-2932 and TMD-8 cells with stable overexpression of IL-16 $\Delta^{511-631aa}$ or EV, 5×10^5 cells/ml, 24h) was collected and used as chemokines. Cell migration of peripheral blood leucocyte (PBLs) is

determined by transwell assay (1h) combined with the CCK-8 test. 10% FBS culture medium were used as control. Rate of chemotaxis (%) = $(OD_{\text{Lower chamber}} - OD_{\text{Background}} / (OD_{\text{Upper chamber}} - OD_{\text{Background}})) \times 100$. (B-D) Migrated PBL is stained with anti-CD3-PE-Cy7, anti-CD4-FITC, anti-CD8-Pacific blue, anti-CD11b-APC-Cy7, and anti-CD14-APC antibodies and analyzed by Flow cytometry to distinguish monocytes, lymphocytes, and granulocytes. (B) the proportion of monocytes, lymphocytes, and granulocytes in migrated PBLs. (C) the proportion of monocytes in migrated PBLs. (D) the proportion of indicated T cells in migrated PBLs. Data shown are mean \pm SD. p values are based on unpaired t-test and Chi-square test. ns=non-significant; *p < 0.05, **p < 0.01, ***p < 0.001, ****p < 0.0001.

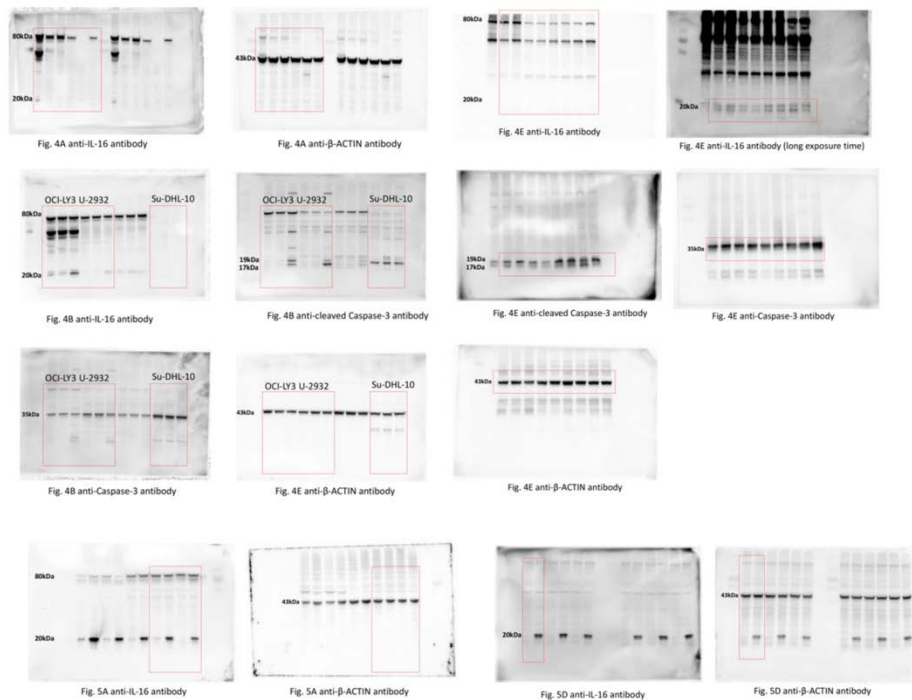


fig. S11. The original images of western blot image in the main article.